The International Journal of Engineering and Science (IJES)
|| Volume || 12 || Issue || 11 || Pages || PP 18-31 || 2023 ||
ISSN (e): 2319 – 1813 ISSN (p): 2319 – 1805

Utilizing Deep Learning Models for the Classification of Thyroid Nodules in Ultrasound Images

Jatinder Kumar
Chitkara University Institute of Engineering and Technology Chitkara University, Punjab, India

Surya Narayan Panda
Chitkara University Institute of Engineering and Technology Chitkara University, Punjab, India

Devi Dayal
Endocrinology and Diabetes Unit, Department of Paediatrics, PGIMER, Chandigarh, India

---*ABSTRACT*---
Thyroid nodules, which are characterized by unusual thyroid cell proliferation, may be a sign of an iodine intake that is too high, thyroid degeneration, inflammation, and other disorders. Although thyroid nodules are mostly benign, the chance that they are cancerous increases considerably each year. Many experiments have been conducted to identify thyroid nodules using deep-learning-based image recognition analysis, reducing the labour of medical professionals and avoiding unnecessary fine needle aspiration and surgical removal. The data was imported directly from the hospitals in Algeria, and volunteer doctors labelled it. There are 1600 photos in total, divided into three categories namely normal thyroid, benign and malignant nodules, where benign referring to less harmful and malignant extremely dangerous thyroid nodules. An assortment of thyroid ultrasound pictures was first subjected to a ResNet50 model that had been previously trained on the ImageNet database. The trained model can now divide thyroid nodules into categories like benign, malignant, and normal. Overall, the suggested model showed that it is possible to identify between benign, malignant thyroid nodules using ultrasound pictures and deep learning.
Index Terms : Benign, Malignant, Alex Net, ResNet-50, Deep Learning.

Date of Submission: 03-11-2023 Date of acceptance: 17-11-2023

I. INTRODUCTION

Thyroid disease is a subset of endocrinology, one of the most significant but underdiagnosed diseases. According to the World Health Organisation (WHO), the two endocrine conditions that are most common around the world are diabetes and thyroid diseases. Approximately 2% and 1% of people are affected by hypothyroidism and hyperthyroidism respectively. Potential causes of hyperthyroidism and hypothyroidism include issues with the thyroid, pituitary, and hypothalamus. Due to a lack of dietary iodine, goitre or active thyroid nodules may develop widespread, with a prevalence of up to 15% in some regions. Endogenous antibodies can injure the thyroid gland, which can contain a variety of cancers and be hazardous (autoantibodies). Early disease identification, diagnosis, and care, according to experts, are crucial for preventing disease progression and even death. Early detection and differential diagnosis boost the likelihood of effective therapy for a variety of illnesses. Clinical diagnosis is typically regarded as a highly challenging process despite several attempts.

The thyroid organ is a butterfly-formed organ organized at the underpinning of the throat. It contains two powerful thyroid synthetic compounds, levothyroxine (T4) and triiodothyronine (T3), which are locked in with mind works, for instance, inner intensity level control, circulatory strain the leaders, and heartbeat rule also thyroid disorder is quite possibly of the most unavoidable sickness all over the planet, and it is generally achieved by an absence of iodine, but it could similarly be achieved by various factors. The thyroid organ is an endocrine organ that secretes synthetics and goes them through the flow framework. It is organized toward the front of the body. Thyroid organ synthetic compounds are obligated for assisting with ingestion as well as staying aware of the body weight, changed, and so on. Thyroid organ prescriptions like T3, T4 and TSH are used to study thyroid activity (thyroid fortifying substance). Thyroid disturbance is requested into two sorts: hypothyroidism and hyperthyroidism. Data mining is a semi-mechanized technique for looking for associations in enormous datasets.

One of the most amazing solutions for several difficult-to-resolve difficulties is AI and profound learning computations. Since AI calculations play a significant role in characterising thyroid infection and because these calculations are high performing and productive, they aid in characterization. Grouping is an information extraction method (AI) used to predict and distinguish numerous illnesses, such as thyroid illness, which we explored and ranked here. Even while the use of computer learning and computerised reasoning in medicine dates back to its inception, there has been another development that has made it necessary to take into account the need for AI driven medical care arrangements. Examiners believe that AI will become commonplace in healthcare sooner rather than later.

However, ultrasound diagnosis mostly relies on the expertise and decision making of medical professionals, which can result in misdiagnosis. ResNet-50 model of Deep learning was used to categorise safe and harmful thyroid nodule. Second, various performance evolution methods were used to illustrate the model's preference for thyroid nodule’s images. The region of interest (ROI) was segmented from the original thyroid ultrasound image for evolution. Finally, we discovered that the properties of thyroid nodules with various characteristics had significantly changed. Overall, the thyroid nodule image ordering achieved using the proposed model.

II. LITERATURE SURVEY

Camargo et al. [1] in this research many strategies and earlier efforts to treat thyroid disease are succinctly discussed. The first sign of a thyroid nodule is the presence of a nodule in the neck region. Of all cancers, thyroid growth has one of the highest incidence rates and has risen the fastest in recent years. The nodules can be located with accuracy using ultrasonography. Thyroid ultrasound images can be examined using a variety of computer-aided diagnosis techniques. Many of these techniques simply use one image for diagnosis rather than all the photos for examination, losing information about the thyroid nodules in the process. It is advised to use several ultrasound images obtained during a checkup to identify thyroid nodules.

Enewold et al. [2] suggested another strategy which directly aggregate the characters that are derived from a wide set of images using an attention-dependent aggregation of features network. It does so in a single examination to increase the precision of identifying malignant nodules. These techniques are used to manually extract and integrate numerous features, making the work challenging.

Russ et al. [3] suggested a model based on inception v3 for identifying thyroid nodule images from the provided dataset. However, they utilised a dataset created by them self that contained fewer training examples. Another strategy is to use the research on computer-aided diagnostics, which automatically distinguishes between benign and malignant nodules from photographs of thyroid nodules. It undergoes numerous processing steps before being utilised to analyse and distinguish between benign and malignant thyroid nodules. There are numerous traits that can be divided into two groups in computer-aided diagnostics. The first is of sonographic quality, whereas the second is not clinical quality. Using data mining and statistical techniques, both were derived from ultrasound pictures.A significant role is played by classifiers, which are frequently utilised in ultrasound-based (CAD) systems. The studies that used characteristics from ultrasound images to categorise thyroid nodules are then looked at, and their shortcomings are highlighted. The methods employed in research that identified thyroid nodules based on non-clinical criteria have also been evaluated and examined.

Xu et al. [4] have used three orthogonal image planes; the method divides US pictures of the breast into four key tissues: fatty tissue, skin, fibro glandular tissue, and mass. The addressed pixel's tissue class inside the image chunk is indicated by CNN. The quantitative criteria for evaluating segmentation outcomes, Accuracy, Precision, Recall, and F1 measure, all above 80%, indicate that the suggested technique is capable of differentiating practical tissues in breast US pictures. The authors concluded that the suggested method has the potential to offer the segmentations needed to aid clinical breast cancer diagnosis and improve imaging in other medical US modes.

Badea et al. [5] scientists used the LeNet CNN design and the Network in Network (NiN) design to categorize blaze photos. The LeNet CNN design was first designed in 1998 for handwritten number detection on banknotes. A nonlinear function approximator that increases the network's capacity for generalization is the multilayer perceptron. The burn picture database had 611 photographs of 53 pediatric patients through a resolution of 1664 × 1248 pixels. Clinical pictures are carefully cropped to a dimension of 230 × 240 pixels. The outcome specified a modest plan executed fine for binary classification difficulties, but as the problems became more complicated, performance dropped substantially.

Poudel et al. [6] utilized various ML techniques to generate more accurate and efficient segmentation, but they necessitate a large number of tagged datasets and a longer training time. According to the authors, 3D U-Net CNN exists as a mechanical subdivision technique for 3-D US pictures that uses a decoder to provide a full-resolution subdivision and an encoder to analyze the whole image by contracting in every succeeding layer. Although it does take additional training time, this technique has the advantage of being able to partition 3D thyroid glands without the usage of handcrafted characteristics. The CNN prototype has the greatest average dice coefficient (DC) of all the segmentation outcomes, at 87.6%. Random forest (RF) and decision tree (DT), which are non-automated segmentation methods, are two other approaches. This approach has a low computing complexity but is sensitive to certain characteristics. The results of the DC, RF, and DT techniques are 86.20 %, 67.00 %, and 86.20 %, correspondingly.

Shenoy et al. [7] have proposed an Improvised U-Net for the probable identification of ROI by segmentation. To achieve greater efficiency, two feature maps, high level, and low level have been explored. The use of these two feature maps helps to avoid low resolution. Further, the Improvised U-Net is tested using the standard dataset DDTI in three sections. First, ROI is compared, which demonstrates that existing models have different ROI than ground models because of limited resolution, but our model has a better ROI. The authors compare the model's True Positive Rate and Dice Coefficient, achieving 98.95 and 95.60, respectively. Furthermore, the model outperforms the previous model by 2.51% and 3.36 %, respectively, according to the comparison analysis. Finally, the author found that, while the Improvised U-Net obtains substantial performance when compared to the present model of segmentation, it can still be improved when batch normalization is taken into account.

Song et al. [8] constructed a backbone convolutional neural network to extract shared feature maps and a classification network to serve as the global branch in a hybrid multi-branch convolutional neural network based on feature cropping. The authors used feature extraction and classified thyroid nodule US images. To lessen the influence of the closeness of local characteristics of benign and malignant thyroid nodule pictures on classification, the researchers introduced a feature cropping branch to the network to perform multi-cropping on batch feature maps. The suggested binary grouping network was then trained using this network. On the DDTI dataset, the suggested method achieved 96.13% accuracy, 93.24% precision, 97.18% recall, and 95.17% F1-measure.

Moussa et al. [9] used a system for classifying thyroid nodules making use of ResNet-50's deep residual network fine-tuning technique. Using pre-trained deep networks enables rapid task learning without the need for millions of images, lengthy training periods, or the definition and training of new networks. This method has the advantage that the pretrained network already contains a substantial collection of attributes that can be used for a number of other jobs. The suggested fine-tuned ResNet-50 model outperforms the VGG-19 model in classifying thyroid nodules, according to experimental results on 814 ultrasound pictures.

Ashok et al. [10] focused on the detection of thyroid cancer utilizing ultrasonic imaging technology's medical images. Those malignant (cancer) bodily components are typically hazy or asymmetrical in ultrasonic imaging. Tumor (cancer) region characteristics closely resemble those of benign or malignant tissues. The use of ultrasound imaging is very important in thyroid diagnosis imaging techniques. Using Python programming and the DDTI dataset, a classification model for more precise diagnosis of papillary thyroid cancer from ultrasound pictures was produced.

Koundal et al. [11] reviewed various methods for automatically classifying thyroid nodules in ultrasound pictures, and determined that CNN performed effectively. The future of diagnostics is the computer-aided diagnosis (CAD).

Albawi et al. [12] the authors have discussed each of the factors that affect network performance. The length of time needed to train the network grows as the number of hidden layers increases because more computations are needed.

Guan et al. [13] used transfer learning by CNN to detect breast cancer from mammograms. Better outcomes were obtained when VGG and neural networks were combined.

Li et al. (14) conducted a small study was conducted by a group of scientists to determine the appropriate classification for identification of thyroid nodules by radiologists and CAD systems. References claim CAD systems outperform radiologists.

Moran et al. (15) it was decided to use CNN to identify thyroid nodules from thermographic images. Three CNN networks (Alex Net, Google Net, and VGG Network) were trained, and their accuracies were determined by comparing their node detection accuracies. The accuracy that was produced by Google Net CNN was the highest (86.22%), followed by Alex Net (77.67%) and VGG (74.96%).

Nguyen et al. [16] utilized both the spatial and frequency domains, and systems-based analysis experiments were conducted. Artificial intelligence was used to locate malignant nodules. It made use of a weighted binary cross-entropy function. Both spatial and frequency domain analyses employing deep learning methods and rapid Fourier-based algorithms were used.

Kwon et al. [17] conducted experiments with 762 photographs to develop a deep-learning algorithm to classify thyroid nodules. Photo overfitting was corrected using the Data Augmentation Approach and Global Average Pooling. The area under the curve (AUC) for the VGG-16 model was calculated to be 0.916.

Liu et al. [18] A novel deep learning-based CAD system was developed in this study, according to the researchers, for autonomous nodule detection and categorization utilizing neural networks. CAD systems typically come in two stages. Pyramidal feature detection was used in the first step to identify nodes, and a multi-branch classification network was used in the second stage to diagnose several views. The two different dataset types each had a detection and diagnosis accuracy of 97.5% and 97.1%, respectively.

Wen et al. (19) Using Tran VGG 19 as a feature extractor, a novel transmission learning method for error diagnosis has been found. Applications like speech recognition, pattern recognition, and image classification all make use of VGG 19. For training, a fully connected layer dropout mechanism was added. The model took 200 seconds to train, and it had a 99.175% accuracy rate.

Ma et al. [20] investigated that fish images are split into six classes when using the Resnet-50 architecture. This was due to the need for a larger database that traditional CNNs cannot access. This method saved time and was 97.19% accurate. The effectiveness of different layers and sample volumes was also evaluated.

He et al. (21), Training deep neural networks has been a challenge. A residual learning architecture was presented to facilitate training. The accuracy of the suggested residual network increased with layer depth, and optimisation was simple. ImageNet and CIFAR-10 records were classified using ResNet Layer 18 and Layer 34 architectures.

Anil et al. [22] investigated risk assessment, and the classification of thyroid nodules was achieved by assessing nodule margin roundness and irregularity using ultrasound and prickle surgery.

Nugroho et al. [23] have proposed a method that could classify thyroid nodules into two groups based on three selected features, round to oval and irregular in shape. The accuracy and specificity of the proposed system were 91.52% and 91.35%, respectively.

Chen et al. [24] have suggested a model distinguish between benign and malignant thyroid nodules in US pictures, as well as to evaluate the kinds of pattern features that may be employed in the development of image pattern classification technologies.

Ding et al. (25) Features were chosen using the lowest redundancy, and maximum relevance method after statistical parameters and the texture of the thyroid lesion area were confirmed using elastography. The SVM classifier was then fed the designated characteristics.

Nanda et al. [26] developed a technique using feature extraction based on local binary pattern variation (LBPV) to distinguish between benign and malignant thyroid nodules with 94.5% accuracy and identify cancerous thyroid nodules.

Rajendra et al. [27] have mentioned that a recent study showed the importance and value of characteristics in computer-generated photographs. The researchers discovered that non-clinical elements, including tissue stiffness scores, texture, and discrete-wavelet-transform-based features, significantly improved classification accuracy when compared to clinical elements like vascularity, edges, shape, microcalcifications, etc.

Further, in [28-29], researchers have used deep learning models using neural networks for efficient predictive model construction for disease identification. Recent research has demonstrated that Deep Convolutional Neural Network (DCNN) picture features can be used to categorize, segment, or retrieve images.

III. PROPOSED SYSTEM

3.1. Implementation Modules:

- **ResNet-50**

ResNet-50, a deep convolutional neural network architecture, was unveiled by Microsoft Research in 2015. It fits to the family of models recognized as ResNet (Residual Network), which is renowned for its ability to train incredibly deep neural networks by minimizing the degradation issue brought on by increasing network depth [30]. **Architecture:** Convolutional layers, shortcut connections, and fully linked layers are among the 50 layers in ResNet-50. ResNet-50 receives a 224x224 RGB image as its input. Following a 3x3 max pooling layer with a stride of 2, the first layer executes a 7x7 convolution with 64 filters. The network is split into four sections, each of which has a collection of leftover blocks. The number of residual blocks varies liable on the stages. Stage 1 has three, Stage 2 has four, Stage 3 has six, and Stage 4 has three. The final step is followed by a fully connected layer with 1000 neurons for classification and a layer that pools global averages.

Residual Blocks: The residual block is the main innovation of ResNet. Two 3x3 convolutions with batch normalisation and ReLU activation make up a residual block. The initial input of the block is combined with the result of the second convolution. The network can learn residual mappings thanks to the shortcut connection, which measures the discrepancy between the input and the desired output. Figure 1 depicts the ResNet-50 architecture. **Bottleneck Architecture:** In the residual blocks of ResNet-50, a bottleneck design is used. The bottleneck architecture keeps performance while lowering computational complexity. ResNet-50 uses three convolutional layers for each residual block: 1x1, 3x3, and 1x1. The feature maps' dimensionality is first decreased by the 1x1 convolutions and subsequently it is raised.

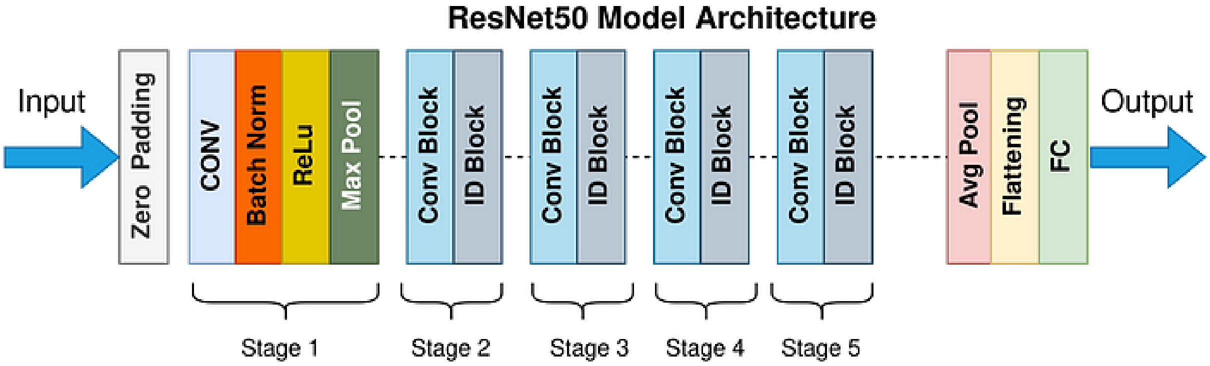

Figure 1: Architecture of ResNet-50

Do Not Connect: Back propagation of gradients is made possible by the use of skip connections, also referred to as shortcut connections. If identity mappings are ideal, the network can learn them thanks to ResNet-50's shortcut connections. By removing the vanishing gradient issue, these connections also make it simpler to train deeper networks. After each convolutional layer, ResNet-50 employs the ReLU activation function. ReLU adds nonlinearity and aids in the network's learning of intricate mappings. **Training:** Stochastic gradient descent (SGD) with a sizable mini-batch size is commonly used to train ResNet-50. A timetable for the learning rate is used to train the network over time. To expand the training set, methods for data augmentation including random cropping and horizontal flipping are frequently used. **Performance:** On a diversity of computer vision jobs, including object detection and image categorization, ResNet-50 has displayed exceptional performance. **ResNet-50** outperformed earlier state-of-the-art models in the ImageNet Large-Scale Visual Recognition Challenge (ILSVRC) 2015 with a top-5 error rate of 7.8%. Because of their breadth, effectiveness, and capacity to get around the difficulties associated with deep neural network training, ResNet-50 and its derivatives have been widely accepted in the field of computer vision.

- **AlexNet**

The development of computer vision and image categorization was greatly aided by the deep CNN architecture known as AlexNet. It was invented by Geoffrey Hinton, Alex Krizhevsky, and IlyaSutskever, and it won the 2012 ILSVRC [31]. One of the first deep neural networks to show exceptional performance in picture classification tasks was AlexNet. **Architecture:** Three completely linked layers and five convolutional layers total eight layers in AlexNet. A 224x224 RGB image is provided to AlexNet as input. 96 filters of size 11x11 with a stride of 4 are used in the first convolutional layer. The second convolutional layer employs 256 filters with a stride of 1 and a 5x5 filter size. A 3x3 max-pooling layer with stride 2 follows the first layer. The third convolutional layer employs 384 3x3 filters. Four and five convolutional layers, respectively, each employ 384 and 256 filters of size 3x3. Each of the completely connected layers has 4096 neurons. Figure 2 depicts the AlexNet architecture. **Activation Function:** Except for the final layer, AlexNet uses the ReLU activation function after each convolutional and fully connected layer. By adding non-linearity, ReLU addresses the vanishing gradient issue. After the first and second convolutional layers, local response normalisation (LRN) is used. The responses of many feature maps at the same spatial position are normalised. Neurons with high relative activations to their neighbours respond better when LRN is present. **Max Pooling:** After the second, fourth, and fifth convolutional layers, max pooling is carried out. The feature maps' spatial dimensions are shrunk, and translational invariance is added. **Dropout:** The completely connected layers are subject to dropout. Each neuron in the completely linked layers is momentarily dropped with a probability of 0.5 during training. Dropout enhances generalisation and prevents overfitting. **Softmax Classifier:** 1000 neurons, or the 1000 classes in the ImageNet dataset, make up the final fully connected layer. The class probabilities are obtained by applying the softmax activation function. **Training:** With a batch size of 128, stochastic gradient descent (SGD) was used to train AlexNet. The learning rate began at 0.01 and was three times reduced by a factor of 10. To expand the training set, methods for data augmentation such cropping and flipping were used. **Performance:** In the ILSVRC 2012 competition, AlexNet outperformed other competitors with a top-5 error rate of 15.3%. AlexNet's accomplishment established the value of deep neural networks for image categorization and opened the door for later developments. Since its debut, the AlexNet architecture has contributed significantly to the advancement of deep learning methods for computer vision problems and served as the basis for numerous cutting-edge CNN models

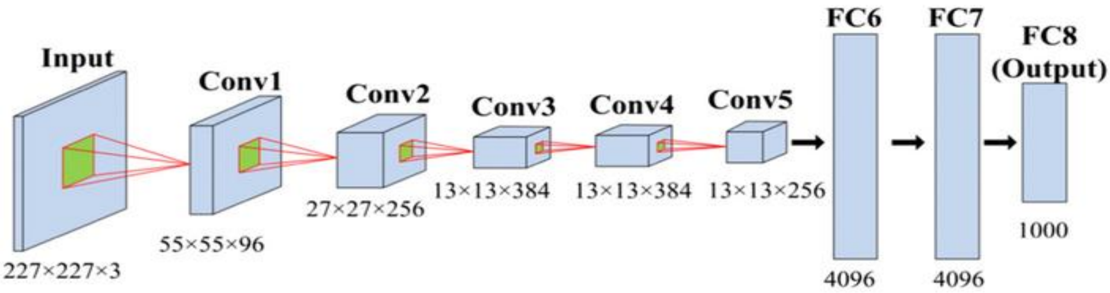

Figure 2: Architecture of AlexNet

In this project, we were gathered 1600 ultrasound images of thyroid nodules of JPG format from the Kaggle and afterward pre-trained them for feasible and optimal classification. Among them, 1280 images of the dataset are saved in a folder and named as train which should be treated as the training set and 320 images are saved in a folder named as test which should be treated as the testing set. Between the training and testing datasets, we made sure that there was no overlapping. If any overlapping occurs, the accuracy increases so there is no point in training the dataset and that's not proper way to train the model. The principal work is as per the following. In the first place, the ResNet-50 model, joined with move learning, was utilized to arrange typical (normal), benign which are harmless and malignant which are dangerous thyroid nodules. Then, the featured areas communicated by Region of Interest (ROI) were distinguished and broke down from distinct images utilizing region-based segmentation and edge detection segmentation techniques. At last, we observed that the qualities of thyroid nodules with various properties were very unique. The accuracy of the AlexNet and proposed model ResNet-50 is 83.59% and 96.20% respectively. In rundown, our technique is compelling in the characterization of thyroid knob pictures.

The work process of thyroid nodule image dataset classification is done with ResNet-50. The Layers and the adaptive pooling depict the course of image by feature extraction and exploration with ResNet-50. With the addition of layers, the key features extricated by the algorithm which turned out to be more dynamic. AUC, the acronym for area under the curve and other examination indexes were utilized to test the effect of training model classification.

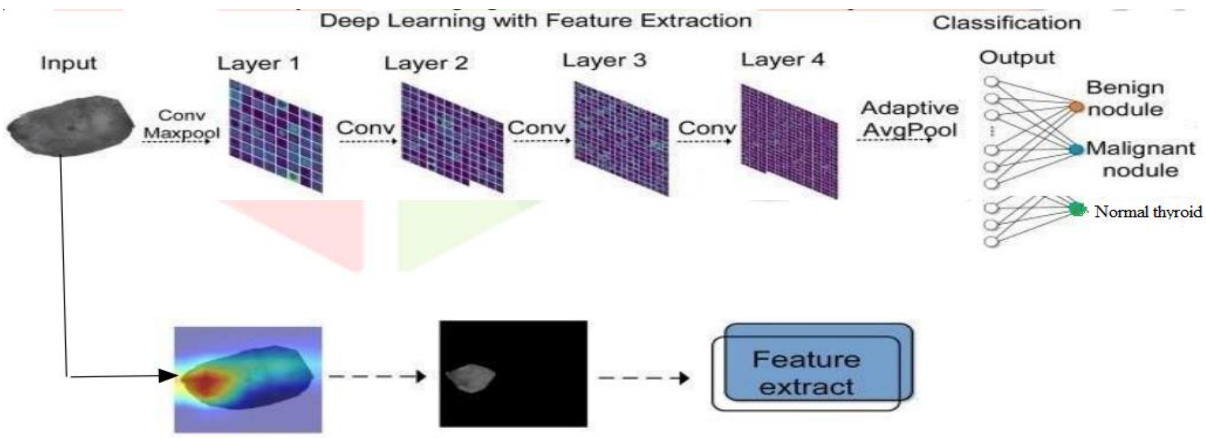

Figure 3 Proposed System diagram

3.2. Data Collection:

The ultrasound images of thyroid nodules have gathered from the Kaggle platform. This image dataset's mode is categorical. The three folders labelled normal, benign, and malignant contain the entire dataset.

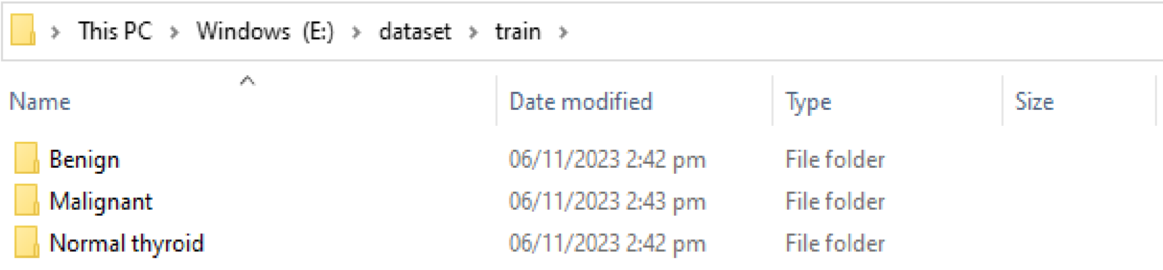

Figure 4: Training Dataset classes.

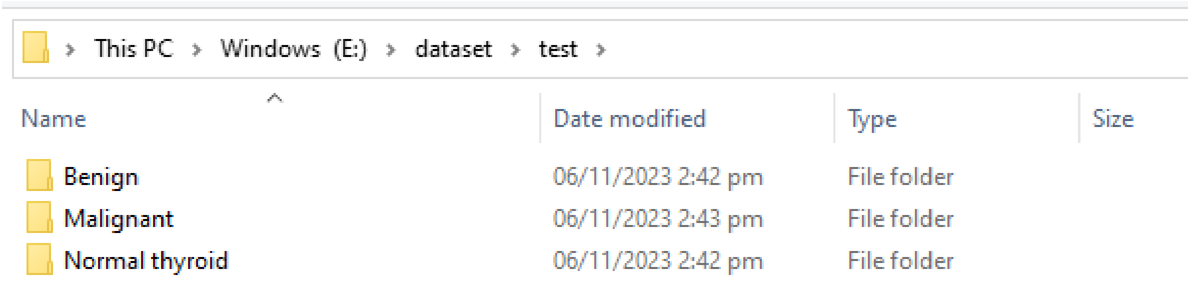

Figure 5: Testing Dataset classes.

Among the ultrasound images from the dataset that fall into the normal category of ultrasound images of thyroid nodules are:

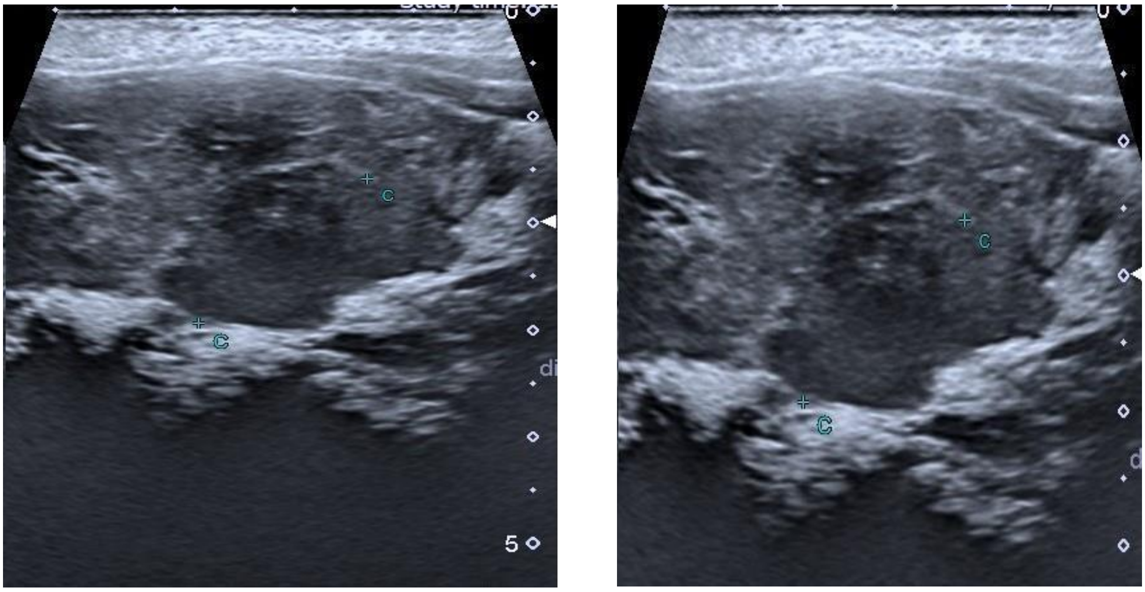

Figure 6: Normal thyroid nodule ultrasound images

Some of the image from the dataset that comes under the benign category of the thyroid nodules ultrasound images is:

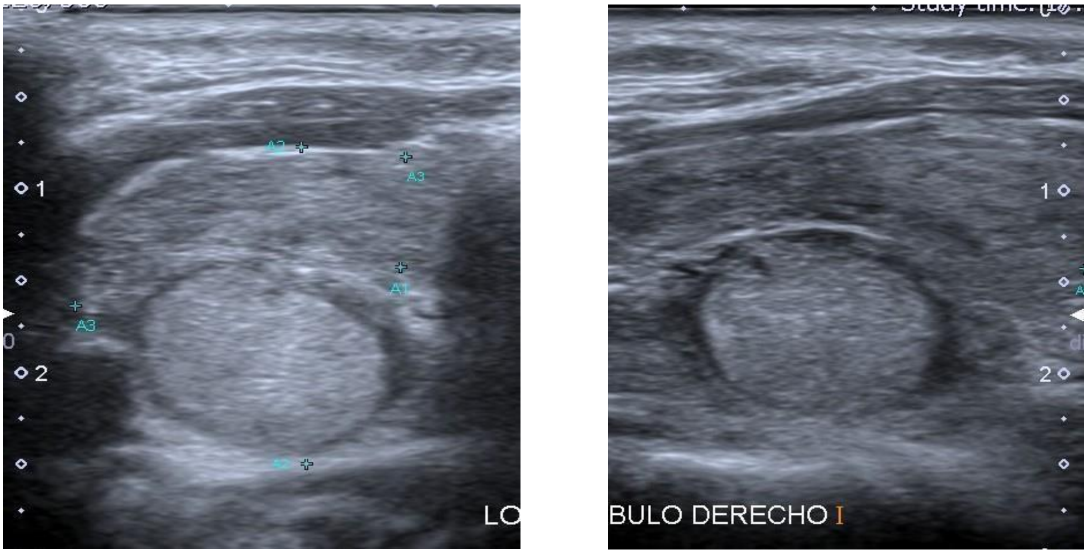

Figure 7: Benign thyroid nodule ultrasound images.

Some of the images from dataset that comes under the malignant category of thyroid nodules ultrasound images:

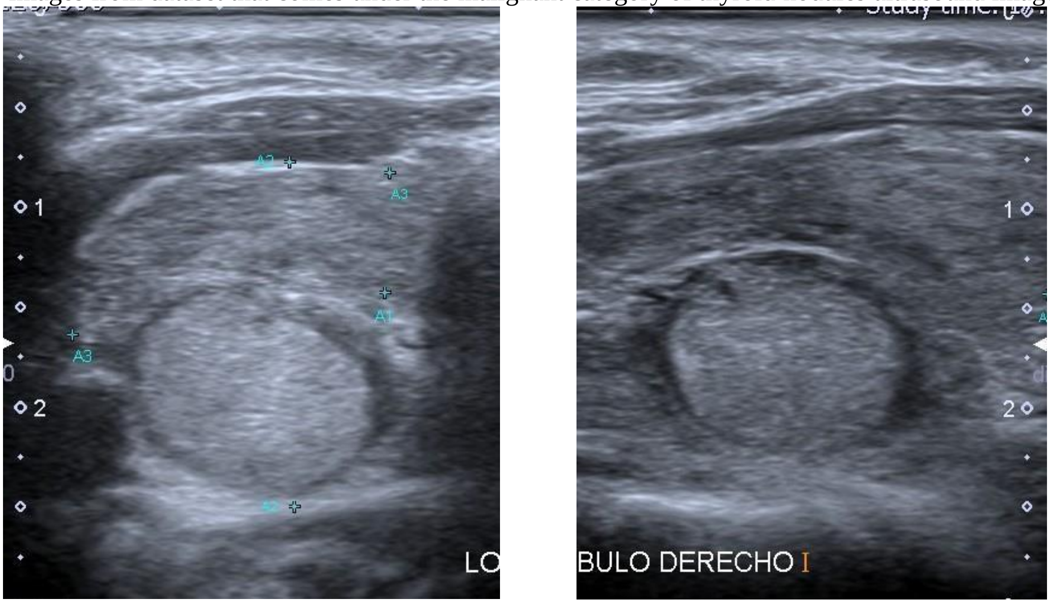

Figure 8: Malignant thyroid nodule ultrasound images.

3.3. Pre-processing of data

Info Pre-processing involves utilising some pre-defined functions built-in Matlab 2021a modules to remove unnecessary frames, sections, and text from the images for improved categorization like color space conversion, contrast enhancement, and morphology etc.

3.4. Splitting of Data

As previously indicated, 1600 photographs were collected from Kaggle; of them, 1280 were utilised to train the model, with the remaining images being used for testing. Given that the dataset mode is categorical, the data was divided at the directory level by putting distinct category photos in the appropriate directories or folders with labels..

3.5. Model Training:

First off, the suggested system makes no mention of the AlexNet model, which we employed. We have utilised AlexNet to demonstrate that the suggested technique provides better accuracy than the current model. Next, we used the suggested technique ResNet-50 to train the dataset.

3.6. Evaluation

The accuracy of the many models that we employed to categorise our dataset is determined in this evaluation phase. We demonstrate that the suggested model performs better than the current model using the evaluation findings.

IV. REQUIREMENT ANALYSIS

Reviewing a few applications' designs to make them more user-friendly is the work at hand. In order to accomplish this, it was essential to preserve organised screen-to-screen navigation while reducing the amount of typing that the user had to do.

REQUIREMENT SPECIFICATION:

Software Requirements

The following are the software requirements for creating the application:

- Operating systems: Ms-Windows 10 or 11
- Matlab 2021a

Hardware Requirements

The following hardware specifications are needed to create the application:
- Core: GPU- NVIDIA if possible
- CPU: Intel Core i7 CPU or higher
- RAM: 32 GB or higher
- Hard Disc Space: 5 TB

V. SYSTEM DESIGN

Data Flow Diagram:

A data flow diagram (DFD) gives an overview of the information flow for any software process or system. It uses pre-defined symbols like rectangles, circles, and arrows along with succinct text labels to show data inputs, outputs, storage places, and paths between each destination. Data flow diagrams shows that it start with input dataset and shows the result as benign, malignant and normal thyroid ultrasound images.

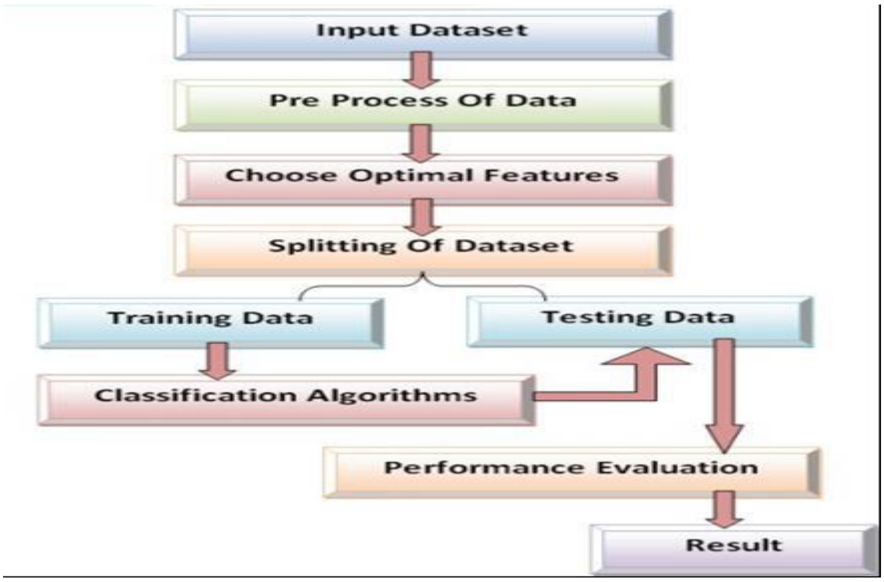

Figure 9: Data Flow Diagram of the proposed system.

VI. EVALUATION DETAILS

6.1. Evaluation metrics

The Evaluation is the process of measuring the quality of a model we have built by using some evaluation metrics like accuracy of the model and ROC curve. We have built two models by using AlexNet and ResNet-50 respectively. The performance of both the models are evaluated based on the evaluation metrics and the best one is selected and used for further classification of thyroid nodules.

6.1.1. Evaluation of AlexNet

Following the AlexNet model training, the model's loss and training accuracy is as follows. Viewing the model loss graph allows one to examine the model's loss and guarantees that the model's loss is reduced during training as shown in figure 10.

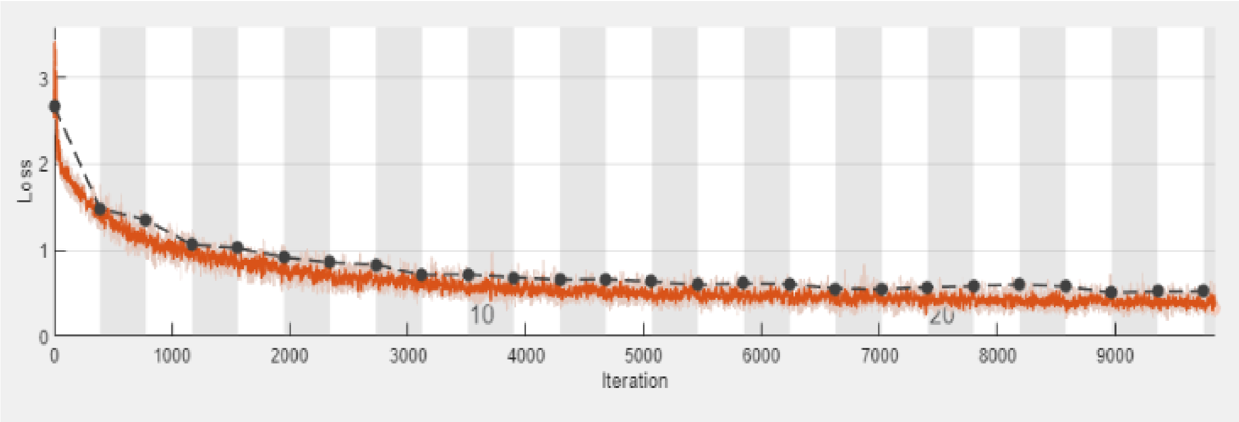

Figure 10: AlexNet Model Loss Graph.

The training graph of AlexNet model is shown in figure 11 and it has been observed that the accuracy improve as the number of iteration increases.

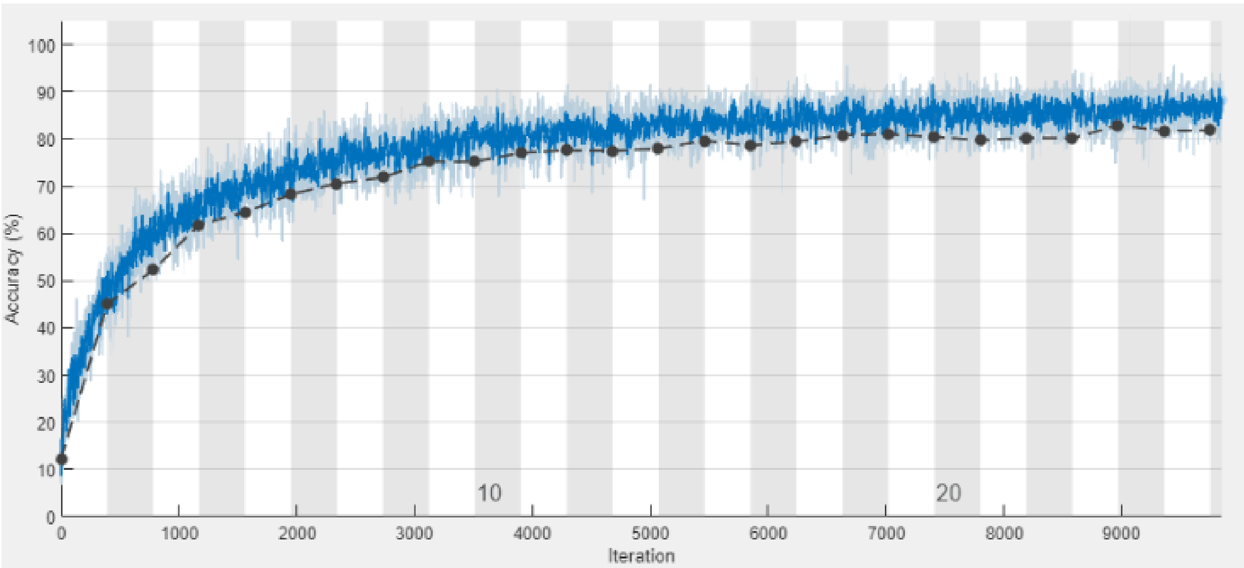

Figure 11: AlexNet Model AUC graph

After the training of the model, the accuracy of the trained model is calculated by providing the explicit testing data set which consists of three classes namely normal thyroid, benign and malignant.

6.1.2. Evaluation of ResNet-50

The model employed this algorithm by inputting the ultrasound images of thyroid. The model Loss and the accuracy curve are depicted in the figure 12 and figure 13 respectively.

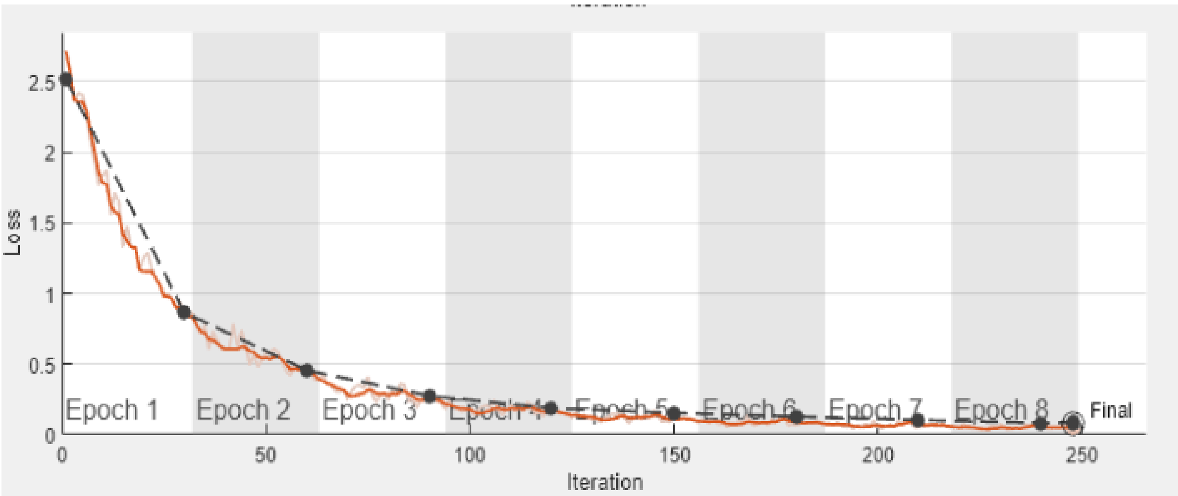

Figure 12: ResNet-50 Model Loss Graph

After the training of the model, to evaluate the performance of the trained model we have calculated the accuracy the model by using the explicit data set which consists of three classes similar to the training dataset. The calculated results are shown below

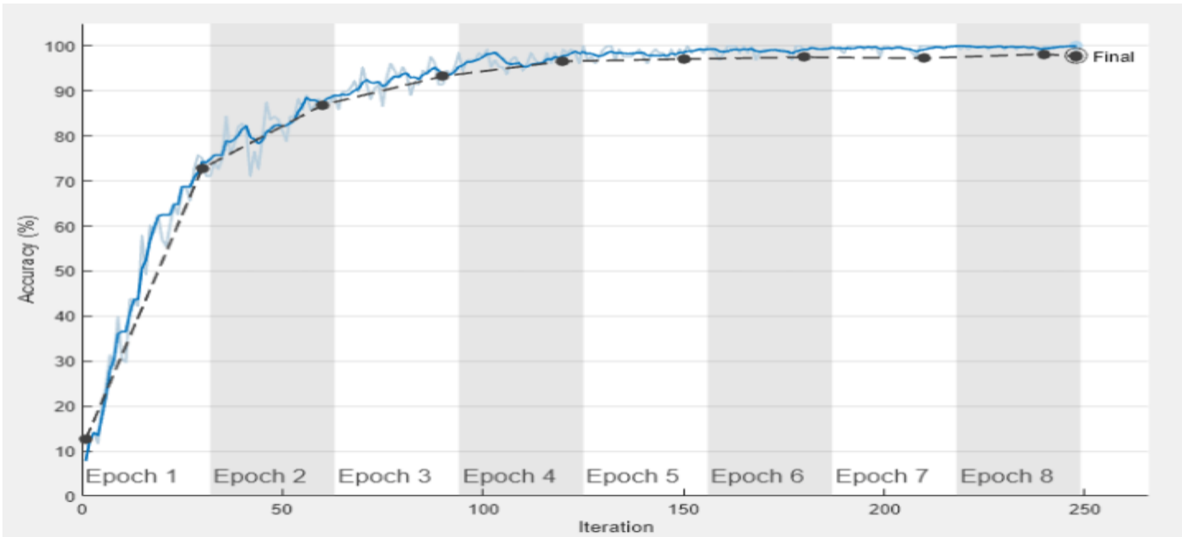

Figure 13: Resnet-50 Model Accuracy.

6.2. Comparision of Algorithms

Here we compare AlexNet and ResNet-50 algorithms and graph is developed based on their accuracies using Ms-Excel. Based on accuracies we have plotted graph against their algorithms and same is shown in figure 14.

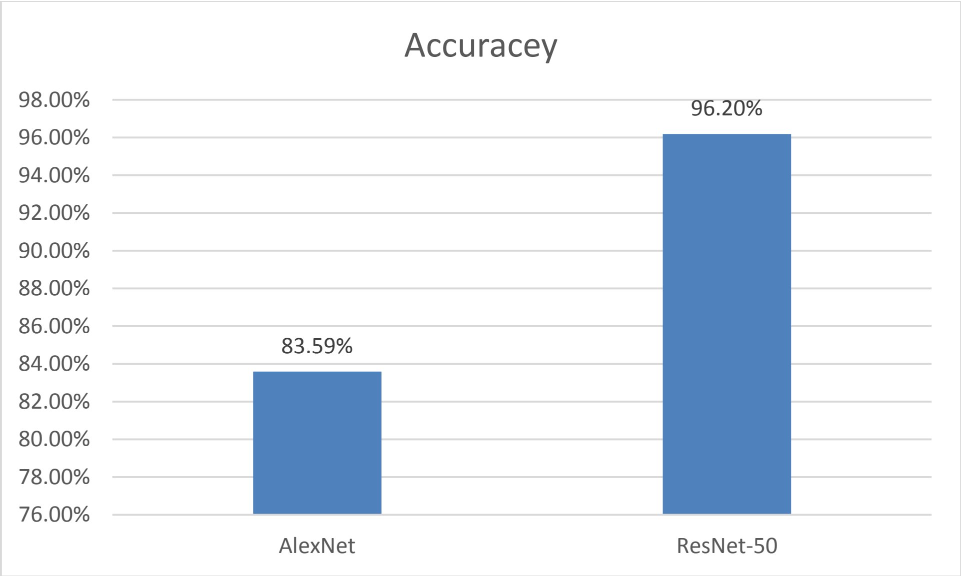

Figure 14: Comparison of Accuracy of models

VII. RESULTS

The user interface has project title followed by a button which redirects to upload thyroid ultrasound. Then followed by another button called "analyze" which shows the final result that whether the uploaded thyroid nodule image is malignant or benign or normal.

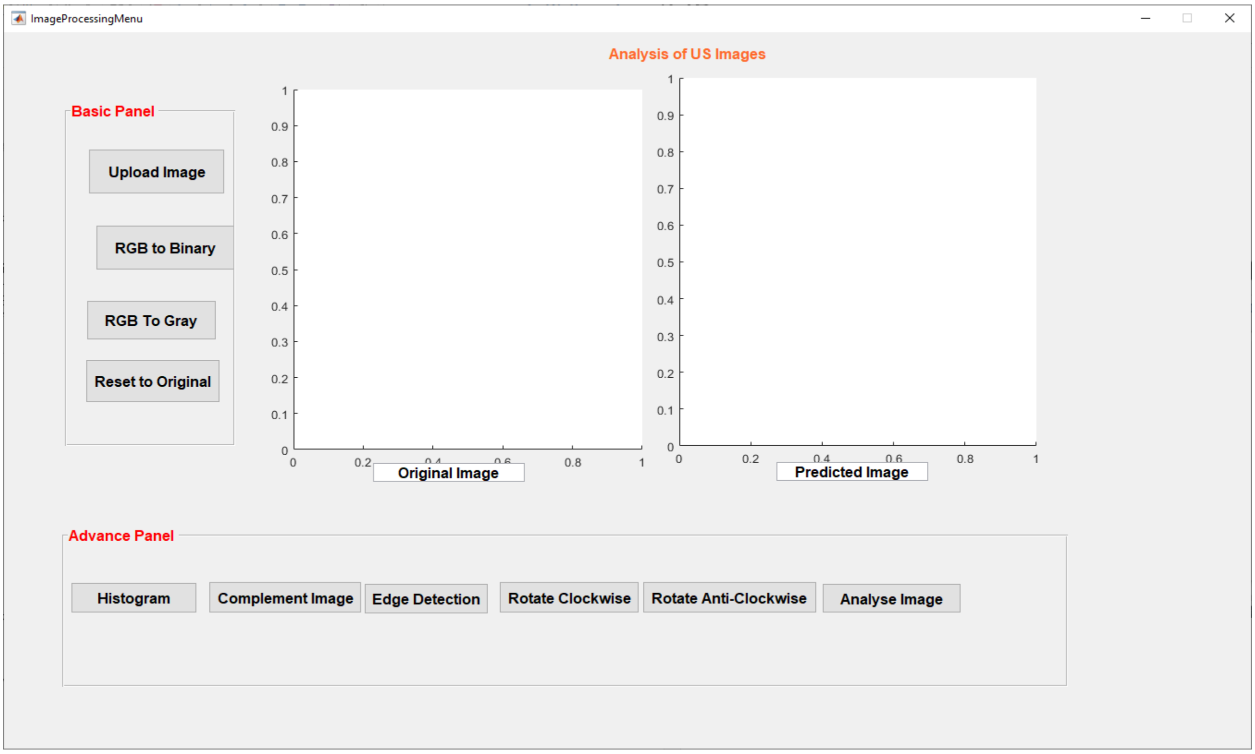

Figure 15: The interface of the proposed framework.

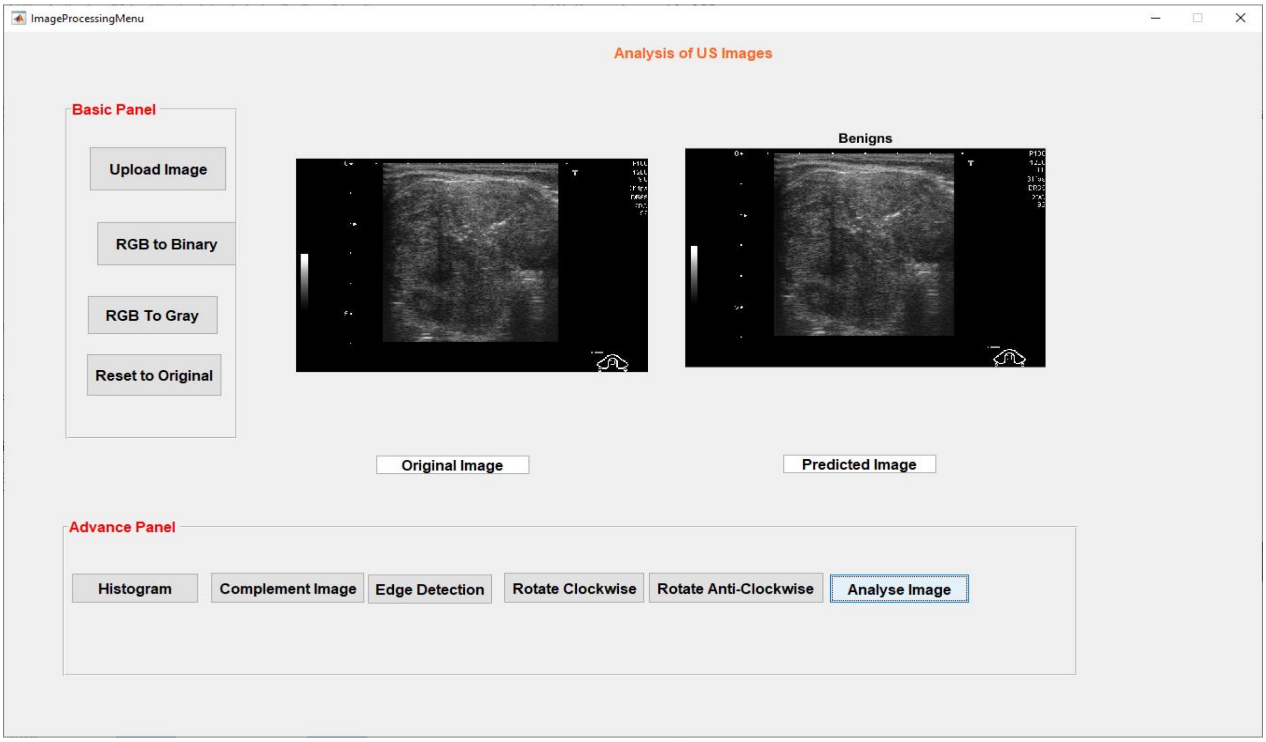

Figure 16: Prediction of Thyroid nodule in the proposed frame work

VIII. CONCLUSION AND FUTURE ENHANCEMENT

A chronic health issue thyroid, an aberrant growth of thyroid cells, needs to be continuously managed. Finding the nodules and classifying them as benign or malignant benefits the patient as well as the physician. This research work titled, Utilizing Deep Learning Models for the Classification of Thyroid Nodules in Ultrasound Images. By applying this model, the doctor can better advise the patient on treatment options and assess the degree of malignancy in the thyroid nodule. A physician can determine if there are a lot of nodules. It provides recommendations while utilising fine-needle aspiration technology.

Thyroid disease affects people of all ages, including children, and is a relatively prevalent condition. Physicians use a variety of conventional methods to find thyroid nodules in patients. Although methods like as Fine Needle Aspiration can identify thyroid in the body, they are extremely damaging to the organism. Examining the patient's ultrasound scans is a safe and alternative course of action. It is suggested to use a deep learning architecture to classify thyroid nodules using ultrasound pictures as input.

The Resnet-50 and AlexNet models were trained and tested using the suggested, improved, and normalised images or dataset. After training, we compared the two models' accuracy, and the model with the better accuracy was used to classify thyroid nodule ultrasound pictures. A user-friendly interface where ordinary people might upload their ultrasound scans and determine if they have thyroid disease or are in a safe zone might be included in further iterations of this concept. It might be made more user-friendly and tailored for hospitals as well as users in order to detect thyroid issues. While aiming for the most precise detection findings, we'll also be trying to increase efficiency.

REFERENCES

[1]. Camargo de, Rosalinda YA, and Eduardo Kiyoshi Tomimori. "Usefulness of ultrasound in the diagnosis and management of well-differentiated thyroid carcinoma." Arquivos Brasileiros de Endocrinologia & Metabologia 51 (2007): 783-792.
[2]. Enewold, Lindsey, Kangmin Zhu, Elaine Ron, Aizen J. Marrogi, Alexander Stojadinovic, George E. Peoples, and Susan S. Devesa. "Rising thyroid cancer incidence in the United States by demographic and tumor characteristics, 1980-2005." Cancer Epidemiology Biomarkers & Prevention 18, no. 3 (2009): 784-791.
[3]. Russ, Gilles, Sophie Leboulleux, Laurence Leenhardt, and Laszlo Hegedüs. "Thyroid incidentalomas: epidemiology, risk stratification with ultrasound and workup." European thyroid journal 3, no. 3 (2014): 154-163.
[4]. Xu, Yuan, Yuxin Wang, Jie Yuan, Qian Cheng, Xueding Wang, and Paul L. Carson. "Medical breast ultrasound image segmentation by machine learning." Ultrasonics 91 (2019): 1-9.
[5]. Badea, Mihai-Sorin, Iulian-Ionut Felea, Laura Maria Florea, and Constantin Vertan. "The use of deep learning in image segmentation, classification and detection." arXiv preprint arXiv:1605.09612 (2016).
[6]. Poudel, Prabal, Alfredo Illanes, Debdoot Sheet, and Michael Friebe. "Evaluation of commonly used algorithms for thyroid ultrasound images segmentation and improvement using machine learning approaches." Journal of healthcare engineering 2018 (2018).

[7]. Shenoy, Nayana R., and Anand Jatti. "Ultrasound image segmentation through deep learning based improvised U-Net." Indonesian Journal of Electrical Engineering and Computer Science 21, no. 3 (2021): 1424-1434.

[8]. Song, Ruoning, Long Zhang, Chuang Zhu, Jun Liu, Jie Yang, and Tong Zhang. "Thyroid nodule ultrasound image classification through hybrid feature cropping network." IEEE Access 8 (2020): 64064-64074.

[9]. Moussa, Olfa, Hajer Khachnaoui, Ramzi Guetari, and Nawres Khlifa. "Thyroid nodules classification and diagnosis in ultrasound images using fine‐tuning deep convolutional neural network." International Journal of Imaging Systems and Technology 30, no. 1 (2020): 185-195.

[10]. Ashok Kumar, Dr Saurabh Mukherjee, Latika Gupta. (2020). "Deep Learning Based Classification Model for Thyroid Malignancy Detection in Ultrasonic Images using Convolution Neural Network". International Journal of Advanced Science and Technology, 29(3), 9566 - 9577.

[11]. Koundal, Deepika, Savita Gupta, and Sukhwinder Singh. "Computer-aided diagnosis of thyroid nodule: a review." International Journal of Computer Science and Engineering Survey 3, no. 4 (2012): 67.

[12]. Albawi, Saad, Tareq Abed Mohammed, and Saad Al-Zawi. "Understanding of a convolutional neural network." In 2017 international conference on engineering and technology (ICET), pp. 1-6. Ieee, 2017.

[13]. Guan, Shuyue, and Murray Loew. "Breast cancer detection using transfer learning in convolutional neural networks." In 2017 IEEE applied imagery pattern recognition workshop (AIPR), pp. 1-8. IEEE, 2017.

[14]. Li, Tingting, Zirui Jiang, Man Lu, Shibin Zou, Minggang Wu, Ting Wei, Lu Wang et al. "Computer-aided diagnosis system of thyroid nodules ultrasonography: Diagnostic performance difference between computer-aided diagnosis and 111 radiologists." Medicine 99, no. 23 (2020).

[15]. Moran, Maira BH, Aura Conci, José R. González, Adriel S. Araújo, W. G. Fiirst, Charbel P. Damião, Giovanna AB Lima, and Rubens A. da Cruz Filho. "Identification of thyroid nodules in infrared images by convolutional neural networks." In 2018 International joint conference on neural networks (IJCNN), pp. 1-7. IEEE, 2018.

[16]. Nguyen, Dat Tien, Jin Kyu Kang, Tuyen Danh Pham, Ganbayar Batchuluun, and Kang Ryoung Park. "Ultrasound image-based diagnosis of malignant thyroid nodule using artificial intelligence." Sensors 20, no. 7 (2020): 1822.

[17]. Kwon, Soon Woo, Ik Joon Choi, Ju Yong Kang, Won Il Jang, Guk-Haeng Lee, and Myung-Chul Lee. "Ultrasonographic thyroid nodule classification using a deep convolutional neural network with surgical pathology." Journal of digital imaging 33 (2020): 1202-1208.

[18]. Liu, Tianjiao, Qianqian Guo, Chunfeng Lian, Xuhua Ren, Shujun Liang, Jing Yu, Lijuan Niu, Weidong Sun, and Dinggang Shen. "Automated detection and classification of thyroid nodules in ultrasound images using clinical-knowledge-guided convolutional neural networks." Medical image analysis 58 (2019): 101555.

[19]. Wen, Long, X. Li, Xinyu Li, and Liang Gao. "A new transfer learning based on VGG-19 network for fault diagnosis." In 2019 IEEE 23rd international conference on computer supported cooperative work in design (CSCWD), pp. 205-209. IEEE, 2019.

[20]. Ma, Yaxin, Pengfei Zhang, and Yunhan Tang. "Research on fish image classification based on transfer learning and convolutional neural network model." In 2018 14th international conference on natural computation, fuzzy systems and knowledge discovery (ICNC-FSKD), pp. 850-855. IEEE, 2018.

[21]. He, Kaiming, Xiangyu Zhang, Shaoqing Ren, and Jian Sun. "Deep residual learning for image recognition." In Proceedings of the IEEE conference on computer vision and pattern recognition, pp. 770-778. 2016.

[22]. Anil, Gopinathan, Amogh Hegde, and FH Vincent Chong. "Thyroid nodules: risk stratification for malignancy with ultrasound and guided biopsy." Cancer Imaging 11, no. 1 (2011): 209.

[23]. Nugroho, Hanung Adi, Anan Nugroho, Eka Legya Frannita, and Igi Ardiyanto. "Classification of thyroid ultrasound images based on shape features analysis." In 2017 10th Biomedical Engineering International Conference (BMEiCON), pp. 1-5. IEEE, 2017.

[24]. Chen, Junying, and Haijun You. "Efficient classification of benign and malignant thyroid tumors based on characteristics of medical ultrasonic images." In 2016 IEEE Advanced Information Management, Communicates, Electronic and Automation Control Conference (IMCEC), pp. 950-954. IEEE, 2016.

[25]. Ding, Jianrui, H. D. Cheng, Jianhua Huang, Yingtao Zhang, and Chunping Ning. "A novel quantitative measurement for thyroid cancer detection based on elastography." In 2011 4th International Congress on Image and Signal Processing, vol. 4, pp. 1801-1804. IEEE, 2011.

[26]. Nanda, S., and M. Mar. "Identification of Thyroid Cancerous Nodule using Local Binary Pattern Variants in Ultrasound Images." Int. J. Eng. Trends Technol 49 (2017): 369-374.

[27]. Acharya, U. Rajendra, G. Swapna, S. Vinitha Sree, Filippo Molinari, Savita Gupta, Ricardo H. Bardales, Agnieszka Witkowska, and Jasjit S. Suri. "A review on ultrasound-based thyroid cancer tissue characterization and automated classification." Technology in cancer research & treatment 13, no. 4 (2014): 289-301.

[28]. Guleria, Kalpna, Shagun Sharma, Sushil Kumar, and Sunita Tiwari. "Early prediction of hypothyroidism and multiclass classification using predictive machine learning and deep learning." Measurement: Sensors 24 (2022): 100482.

[29]. Sharma, Shagun, Kalpna Guleria, Sunita Tiwari, and Sushil Kumar. "A deep learning based convolutional neural network model with VGG16 feature extractor for the detection of Alzheimer Disease using MRI scans." Measurement: Sensors 24 (2022): 100506.

[30]. Russakovsky, Olga, Jia Deng, Hao Su, Jonathan Krause, Sanjeev Satheesh, Sean Ma, Zhiheng Huang et al. "Imagenet large scale visual recognition challenge." International journal of computer vision 115 (2015): 211-252.

[31]. He, Kaiming, Xiangyu Zhang, Shaoqing Ren, and Jian Sun. "Deep residual learning for image recognition." In Proceedings of the IEEE conference on computer vision and pattern recognition, pp. 770-778. 2016.